

AN X-BAND GUN TEST AREA AT SLAC

C.G. Limborg-Deprey*, C. Adolphsen, S. Chu, M. Dunning, K. Jobe, E. Jongewaard, C. Hast, A.E. Vlieks, F. Wang, D. Walz, SLAC National Accelerator Laboratory, Menlo Park, CA, 94025
R.A. Marsh, S.G. Anderson, F.V. Hartemann, T. Houck, LLNL, U.S.A.

Abstract

The X-Band Test Area (XTA) is being assembled in the NLCTA tunnel at SLAC to serve as a test facility for new RF guns. The first gun to be tested will be an upgraded version of the 5.6 cell, 200 MV/m peak field X-band gun designed at SLAC in 2003 for the Compton Scattering experiment run in ASTA [1]. This new version includes some features implemented in 2006 on the LCLS gun such as racetrack couplers, increased mode separation and elliptical irises. These upgrades were developed in collaboration with LLNL since the same gun will be used in an injector for a LLNL Gamma-ray Source [2,3]. Our beamline includes an X-band acceleration section which takes the electron beam up to 100 MeV and an electron beam measurement station. Other X-Band guns such as the UCLA Hybrid gun [4] will be characterized at our facility.

RF

Gun RF Design

Modifications were included to the Compton gun version [1] in a similar way as was done for the LCLS gun [5,6] from the SLAC/BNL/UCLA 1.6 cell S-Band gun. A racetrack shape for the coupling cell was implemented to suppress the quadrupole component introduced by the dual feed. The original racetrack shape calculation was described in [7]. The improvement to the transverse emittances were calculated in [8]. The gun is tuned to have the π -mode at 11.424 GHz. The other modes are undesired since their excitation can degrade the energy stability. The frequency separation of the nearest resonant mode was increased from 8.5 MHz in the early version to 25 MHz by opening slightly the iris. The iris was made elliptical in order to reduce the local surface electric field amplitude to a value lower than that on the cathode.

With an iris radius of $a=4.67$ mm, the a/λ ratio is 0.178. The coupling cell ports were designed to give a beta coupling coefficient of ~ 1.7 to reduce the filling time constant to 80 ns and consequently the peak rf pulse heating. At steady state, rf power of 17 MW will provide the required 200 MV/m peak field on the cathode.

A pulse heating calculation indicated a maximum temperature rise of 50 deg C for a 17 MW, 180 ns square input rf pulse. This heating is just at the acceptable level.

Work supported by the U.S. Department of Energy under contract DE-AC02-76SF00515.

*corresponding author: limborg@slac.stanford.edu

Operation of the gun at 60 Hz with 180 ns long RF pulses will generate 330 W to be removed by the water cooling system. With an approximate 10 psi pressure drop, the water flow velocity will be 3.37 m/s in the single cooling channel, the film temperature drop will be 4 deg C and the water temperature increase along the gun will be 0.6 degC. We will regulate the copper temperature to the 0.1deg C level. A 0.1deg C temperature variation gives a phase shift of 0.5 deg X-Band.

RF Distribution

A SLED-II system will compress 50 MW, 1.5 μ s RF klystron pulses to 200 MW, 250 ns pulses. A high power H-hybrid type 6 dB divider will send $\frac{1}{4}$ of the power to the RF gun and the rest to the linac section. A T105 linac section approximately 1 m long will accelerate the electron beam from the RF gun exit to approximately 100 MeV. A high power RF attenuator and phase shifter comprised of two H-hybrids and two WC150 phase shifters will allow phase and amplitude adjustment of the RF to the gun [7]. Another WC150 phase shifter will give independent control of the relative phase between the RF gun and T105, offering high flexibility for tuning. Another separated high power RF station without pulse compression will be available in the future to supply the necessary RF power to an X-Band transverse deflecting cavity, which requires 17 MW for a 3 MV integrated transverse kick.

BEAM DYNAMICS

X-Band vs S-Band

The 5.6 cell X-Band gun was studied for a variety of charges and peak voltages. Particular interest was given to the optimization at 250 pC as it corresponds to the nominal charge for the LCLS operation. A 200 MV/m peak voltage has been assumed as of now for our X-band gun since it was successfully operated at that voltage before [1]. The LCLS gun routinely operates at 115 MV/m. We compute that our XTA beamline can deliver 250 pC with a transverse emittance $\epsilon_{x,95\%} \sim 0.25$ mm-mrad, thus smaller than the 0.4 mm-mrad routinely measured in the LCLS injector and an rms bunch length of 0.76 ps, thus 3 times shorter than the LCLS one. As can be seen in Figure 1, the longitudinal electric field seen by the electron over the first mm is 2-3 times larger than that seen by the electrons in the S-Band gun. A relativistic beta of 0.5 is reached in 1 mm, whereas it is reached in 3 mm for the S-Band 1.6 cell gun.

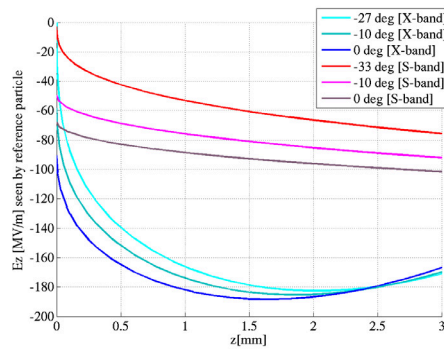


Figure 1: Longitudinal electric field seen by particle for a 1.6 cell S-Band gun [red] and the 5.6 cell X-Band gun [blue]. Zero degrees correspond to on-crest at the gun exit.

Gun Performance

The optimum injection phase for the 5.6 cell version is 18 degrees from the zero-crossing. At this value, the field on the cathode is approximately 60 MV/m. This is similar to the field seen at emission in the LCLS gun operated at 115 MV/m, 30 degrees from the zero-crossing. Accordingly, QE and thermal emittance should be similar to those measured on the LCLS gun. For the 5.5 cell version, the optimum injection phase is closer to 30 deg. In simulations, both the 5.5 and 5.6 cell versions seem to deliver similar beam performances for 200 MV/m and 250 pC when assuming an identical thermal emittance. However, the thermal emittance increases with cathode voltage [9], so the 5.6 cell version might perform slightly better than the 5.5 cell in terms of transverse emittances. On the other hand, the 5.6 cell gun will be prone to more charge jitter as operation at 15 deg from zero crossing implies 3% charge fluctuation per deg X-Band against 1.5% at 30 deg.

Table 1: Results From Optimizations of the XTA beamline.

Q [pC]	$\epsilon_{x,100\%}, \epsilon_{x,95\%}$ [mm-mrad]	σ_1 [mm]	$Q/\sigma_1/\epsilon / 1e3$
250	0.38/0.25	0.228	4.39
250	0.42/0.28	0.184	4.85
100	0.362/0.265	0.116	3.25
20	0.1/0.075	0.109	2.44
10	0.070/0.052	0.105	1.83
10	0.092/0.076	0.055	2.39
10	0.140/0.118	0.042	2.01
1	0.022/0.016	0.080	0.78
1	0.042/0.036	0.025	1.11

Operation at Low Charge

Table 1 shows results obtained for different charge levels when running the 5.6 cell gun with a 200 MV/m peak voltage. The initial distribution was either a single or dual gaussian with 30 to 100 fs rms lengths, depending on the charge, and a flat top transverse profile. A real blow-out regime simulation would use a parabolic transverse

profile. Slightly better numbers might thus be obtained than those presented in table 1. All simulations results presented in this paper were computed with ASTRA [10]. The third optimization studied for 10pC gives an rms bunch length of 42 μm . It was used in a start-to-end calculation [11] for an X-Band driven XFEL delivering 2.3 fs fwhm electron pulses at 6 GeV for SASE lasing at 20 GW peak power. In this proposed design, the accelerator is 200 m long. It includes two compressors and has no linearizer.

Operation at Reduced Fields

To mitigate possible high dark current issues, and with a view to run with higher repetition rates, we investigated the optimization of this gun for lower peak voltages. Figures 2a and 2b show that very good emittances and relatively small bunches could still be obtained at lower peak voltages. The computation was done for 100 pC. For 100MV/m peak voltage, a 5.4 cell gun would perform better than the 5.5 and 5.6 cell guns [12].

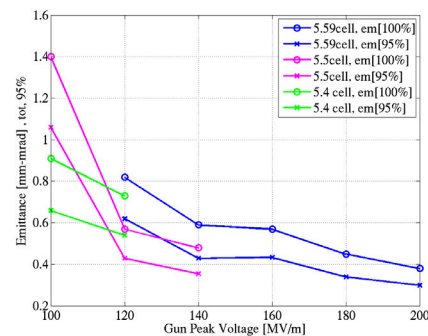


Figure 2a: Transverse emittance for reduced peak voltage.

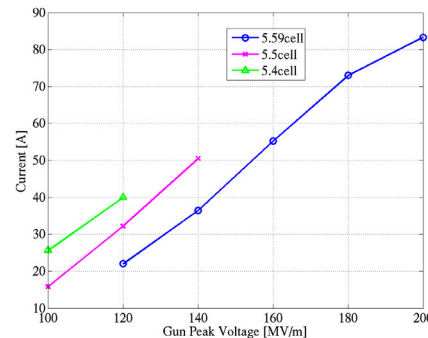


Figure 2b: Peak current for reduced peak voltage.

BEAMLINE LAYOUT

The XTA beamline will be installed in a 6.7 m region at the downstream end of the NLCTA tunnel. The gun, GTL (gun-to-linac) and T105 accelerator will use 1.7 m leaving 5 m for a beam characterization station.

GTL Diagnostics

The GTL section has to be very short (<0.6 m) for optimum emittance compensation. But it should accommodate vacuum pumping, steering, a port for injection laser, a screen and a cavity BPM upstream of the T105 entrance. There is no space for a spectrometer. The

energy at the gun exit will be inferred from the rotation of patterns imaged onto a screen. Such a measurement relies on a good solenoid calibration. Point-to-point imaging is possible at 200 MV/m onto a screen located at 0.5 m from the cathode, but with a demagnification of 0.2.

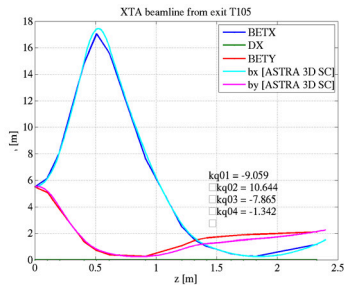


Figure 3a: optics tuning 1 for quad scan at screen S1.

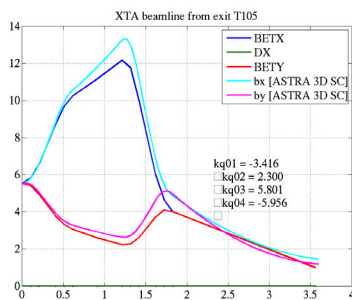


Figure 3b: optics tuning 2 for quad scan at screen S2.

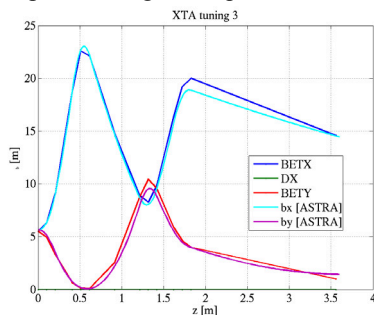


Figure 3c: optics tuning 3 for quad scan at screen S2-space charge can be neglected in data processing.

100 MeV Diagnostics

The diagnostics section starts with 2 pairs of 2 quadrupoles, between which is installed an 11 cell X-Band transverse deflecting cavity (TD11). Downstream of these quadrupoles, beam sizes will be measured on a screen S1 located just in front of a spectrometer. With the optics tuning shown in Figure 3a, one can measure the transverse emittance by performing a quadrupole scan with the second quadrupole. However a full simulation of the quadrupole scan performed with ASTRA-3D [10] for 250 pC shows that the emittance calculated in mm-mrad gives a value of 0.8 instead of 0.65 for the particular case of 250 pC. The transport matrices will have to include a space charge term [13]. A second screen S2 is located in the straight ahead beamline and will be run with the spectrometer turned off. Both planes can be measured at the same time. For the optics tuning shown in figure3-b, the space charge effects, even if reduced compared to

those present in optics tuning 1, have to be taken into account. If they are ignored the emittances in mm-mrad are wrongly evaluated to be 0.61 and 0.69 instead of 0.65. With the optics tuning shown in Figure 3c, the reconstruction of emittance from the quadrupole scan performed with the fourth quadrupole does not require including the space charge terms into the transport matrix. However to compute the twiss parameters at the exit of the linac section, one will still need to include the space charge term in the matrices representing the transport through the low betatron function region at 0.6 m. Also, in this configuration, only one plane can be measured at a time. In the three optics tunings discussed above there is a 90 phase advance from the transverse deflecting cavity to the measurement screen. For optics tuning 2, the resolution of the bunch length scales like $33\text{fs} \cdot \sqrt{\epsilon_n} / V[\text{MV}]$ with V the integrated kick voltage, ϵ_n the normalized emittance and a betatron function of 11m at the transverse deflecting cavity. An integrated kick of 3 MV will be available. The energy spread generated at the transverse cavity is proportional to $10\text{keV} \cdot V[\text{MV}] \cdot \sqrt{\epsilon_n}$ when the betatron function at TD11 is 0.25 m as in optics tuning 1.

REFERENCES

- [1] A.E. Vliet, et al. "Recent measurements and plans for the SLAC Compton X-ray source", SLAC-PUB-11689, 2006. 10pp. Published in AIP Conf.Proc.807:481-490,2006
- [2] R.Marsh "X-Band RF Photoinjector research and development at LLNL" TUP023, these proceedings
- [3] S.Anderson et al. "VELOCIRAPTOR: an X-band photoinjector and linear accelerator for the production of mono-energetic γ -rays" Submitted to NIM A, Proceedings of XB10, Daresbury UK, 2010.
- [4] A.Valoni et al. "RF properties of a X band hybrid photoinjector", Proc. of XB10, Daresbury UK, 2010.
- [5] C.Limborg et al. "RF Design of the LCLS GUN", <http://www-ssrl.slac.stanford.edu/lcls/technotes/lcls-tn-05-3.pdf>
- [6] L. Xiao, "Dual Feed RF Gun design for the LCLS", Proceedings of 2005 Particle Accelerator Conference, Knoxville, Tennessee
- [7] C. Nantista et al., "Low-field accelerator structure couplers and design techniques", Phys. Rev. ST Accel. Beams 7, 072001, 2004
- [8] F.Zhou, et al "X-band Photoinjector Beam Dynamics", IPAC-2010-TUPECO22, May 2010.
- [9] D. H. Dowell, J.Schmerge "Quantum Efficiency and Thermal Emittance", Phys. Rev. ST Accel. Beams 12, 074201 (2009)
- [10] K. Floettmann, ASTRA, http://www.desy.de/~mpyflo/Astra_dokumentation
- [11] Y.Sun, C.Limborg, J.Wu "A hard X-ray FEL design based on all x-band accelerator", submitted to PRST-AB
- [12] C.Limborg et al, "X-Band gun for high repetition rate" to be published in NIM
- [13] C.Limborg et al, "A Modified QuadScan Technique for Emittance Measurement of Space Charge Dominated Beams", WGG03, PAC03 Portland